BULLETIN OF THE EARTHQUAKE
RESEARCH INSTITUTE
Vol. 45 (1967), pp. 375-393

22. *Studies of the Thermal State of the Earth. The 21st Paper: Heat-Flow, Eastern Pacific**.

By Victor VACQUIER, John G. SCLATER and Charles E. CORRY,**

Marine Physical Laboratory of the Scripps Institution of Oceanography, University of California, San Diego.

(Read July 19, 1966.—Received March 31, 1967.)

Abstract

One hundred and ninety-seven new heat-flow measurements taken by Scripps Institution of Oceanography in the east Pacific Ocean off the coast of North and Central America are presented. These and three hundred and sixty-seven previous measurements taken in the eastern Pacific Ocean, east of 140°W and between 60°N and 10°S are used to describe the regional pattern of the area. A contour map is presented. The eastern Pacific Ocean is divided into three distinct regions: the area north of 25°N comprising the Mason-Raff magnetic lineations, a second region comprising the California Seamount Province, the East Pacific Rise, the Gulf of California, and the eastern Pacific Ocean basin, and finally a third area east of 100°W which encompasses the Middle America Trench, the Cocos, Galapagos and Carnegie ridges, the Galapagos Platform and the Guatemala Basin. An analysis is made of the heat-flow measurements in each area. This analysis shows that in the second and third regions, large areas exist having an average outward flow of heat greater than 3.0 μcal/cm^2/sec, the oceanic average is 1.58 μcal/cm^2/sec (Lee and Uyeda, 1965). These areas which are adjacent to equally large areas of subnormal heat-flow are in striking contrast with the uniformity of heat-flow which has recently been discovered in the northwest Pacific basin and seems to be typical of other ocean basins. It is unlikely that the distribution of these areas of high and low flow east of the East Pacific Rise can be explained by large-scale thermal convection cells in the mantle.

---

* Contribution from the Scripps Institution of Oceanography, University of California, San Diego.

** Communicated by T. Rikitake.

1. Introduction

During the past fifteen years more than 500 heat-flow measurements have been made in the east Pacific Ocean off the coast of Central and North America. Previous measurements have been reported by Bullard (1954), Bullard, *et al.* (1956), Maxwell (1958), Von Herzen (1959, 1960, 1963), Foster (1962), Von Herzen and Uyeda (1963), Von Herzen and Maxwell (1964), and Langseth, *et al.* (1965). A full listing of these measurements can be found in Lee and Uyeda (1965).

Since January 1965, 197 new heat-flow measurements have been taken in the Pacific east of 140°W and north of 10°S, during five expeditions of the Scripps Institution of Oceanography. On the first of these expeditions, Argo 3-65, 37 stations were taken in a closely spaced area across two prominent north-south Mason-Raff magnetic lineations. These measurements investigated the possible correlation between heat-flow and the highs and lows in the magnetic anomalies. During expedition Papagayo, 97 heat-flow measurements were obtained. Almost all were situated in or around the Middle America Trench. Early in the following year, 4 heat-flow stations were occupied on the East Pacific Rise during the last leg of the first cruise of the THOMAS WASHINGTON. The last leg of expedition Zetes contributed a futher 13 stations in this area and, finally, late in 1966, 50 heat-flow stations were successfully occupied during expedition Tripod—a magnetic, heat-flow and gravity survey of three areas in the eastern Pacific.

2. Results

A summary of the results and the positions of the stations from the present work is given in Table 1. The values range from a high of 6.3 μcals/cm^2/sec near the Mathematician Seamounts to a low of 0.1 μcal/cm^2/sec at the boundary of the Cocos Ridge and the Middle America Trench. The station positions were determined by astronomical methods except for a few stations near the continental United States which had their positions determined by Loran. An account of the apparatus used in making these heat-flow stations can be found at the end of this paper. Fig. 2 presents a chart showing the position of these and other published and unpublished values in the eastern Pacific.

3. The Contour Chart

Before a contour interval can be selected with any feeling of re-

Table 1. New Heat-Flow Measurements, Eastern Pacific

Station No.	Position		Water Depth, meters	Thermal Gradient	K	Q	Tilt	Penetration
	Latitude	Longitude		Average				
	N	W		$\times 10^3$ °C cm^{-1}	$\times 10^3$ cal °C^{-1} cm^{-1}sec^{-1}	$\times 10^6$ cal cm^{-2} sec^{-1}	Degrees	cm
				Expedition Argo-3-65				
1	32°07′	120°39′	3746	0.94	2.1 a	2.0		f
2	32°06′	121°28′	3973	0.62	2.1 a	1.3		f
3	32°12′	122°51′	4249	0.82	1.78n	1.46		f
5	32°17′	123°56′	4307	0.47	2.18n	1.02		f
6	32°37′	124°15′	4432	0.18	2.11n	0.38		f
7	32°38′	124°27′	4360	1.20	2.03n	2.44		f
8	32°37′	125°15′	4493	0.97	2.04n	1.98		f
9	32°15′	125°13′	4417	0.32	2.05n	0.66		f
10	32°13′	125°57′	4188	0.99	2.05n	2.03		f
11	32°30′	125°52′	4284	1.00	2.05n	*2.05*		106
12	32°37′	126°12′	4410	0.63	2.28n	1.44		f
13	32°31′	126°27′	4295	0.98	2.17n	2.13		f
14	32°30′	127°06′	4421	0.82	2.00n	1.64		f
15	32°40′	127°14′	4410	0.54	2.11n	1.14		f
16	32°41′	127°02′	4410	0.64	2.17n	1.39		f
17	32°40′	126°48′	4341	0.97	2.1 a	2.0		f
18	32°39′	126°43′	4322	1.09	2.1 a	2.3		f
19	32°35′	126°35′	4379	0.97	2.1 a	2.0		f
20	32°52′	126°28′	4303	1.05	2.1 a	2.2		f
21	33°01′	126°52′	4226	0.86	2.1 a	1.8		f
22	32°37′	126°53′	4448	0.79	2.1 a	1.7		f
23	32°14′	125°10′	4356	0.23	2.1 a	0.5		f
24	32°21′	125°32′	4379	0.94	2.1 a	2.0		f
25	32°29′	125°57′	4303	1.43	2.1 a	3.0		f
26	32°28′	126°16′	4394	1.06	2.1 a	*2.3*		100
27	33°17′	126°20′	4379	1.11	2.1 a	2.3		f
29	34°01′	126°23′	4780	0.67	2.1 a	1.4		f
30	34°30′	126°29′	4680	1.21	1.96n	2.37		f
31	34°30′	126°06′	4649	1.41	2.01n	2.85		f
32	34°32′	125°31′	4626	1.05	2.1 a	2.2		f
33	34°34′	125°58′	4493	1.05	2.1 a	2.2		f
34	34°37′	124°23′	4379	0.25	2.1 a	0.5		f
35	35°11′	124°36′	4417	0.60	2.1 a	1.3		f
37	33°47′	125°21′	4226	0.05	2.1 a	0.1		f
38	33°45′	125°50′	4303	0.31	2.1 a	0.7		f
39	33°37′	126°07′	4238	0.94	2.1 a	2.0		f
40	33°27′	126°24′	4257	0.73	2.1 a	1.6		f
				Expedition Papagayo				
1	07°46′	82°42′	1838	0.91	1.8 a	1.6		f
2	07°06′	82°32′	3425	2.17	1.8 a	3.9		f
3	07°12′	82°01′	2076	1.26	1.8 a	2.3		f
4	05°18′	81°54′	3894	2.20	1.79n	3.95		f
5	04°28′	81°36′	3380	1.96	1.8 a	3.5		f
6	05°38′	82°51′	3380	2.18	1.8 a	3.9		f
7	06°51′	83°17′	2241	2.30	1.8 a	4.1		f
8	07°51′	85°11′	2505	0.05	1.8 a	0.1		f

(to be continued)

Table 1. (continued)

Station No.	Position		Water Depth, meters	Thermal Gradient	K	Q	Tilt	Penetration
	Latitude	Longitude		Average				
	N	W		$\times 10^3$ °C cm^{-1}	$\times 10^3$ cal °C^{-1} cm^{-1}sec^{-1}	$\times 10^6$ cal cm^{-2} sec^{-1}	Degrees	cm
9	08°03′	85°32′	2854	0.14	1.8 a	0.3		f
10	08°39′	85°44′	2947	2.23	1.8 a	4.0		f
11	09°02′	84°48′	2078	0.71	1.8 a	1.3		f
12	08°27′	84°27′	2481	3.18	1.8 a	5.8		f
13	08°14′	83°33′	1936	1.17	1.8 a	2.1		f
14	08°04′	84°58′	2539	1.76	1.8 a	3.2		f
15	07°42′	85°43′	2987	1.40	1.8 a	2.5		f
16	08°18′	85°49′	2951	1.96	1.8 a	3.5		f
17	08°46′	86°12′	3239	1.90	1.8 a	3.4		f
18	09°37′	86°07′	4170	0.05	1.8 a	0.1		f
19	10°02′	86°07′	1815	0.38	1.8 a	0.7		f
20	10°12′	86°45′	4402	0.64	1.8 a	1.2		f
21	09°57′	87°00′	3132	0.37	1.8 a	0.7		f
22	09°37′	87°22′	3220	0.40	1.8 a	0.7		f
23	09°03′	87°51′	3371	0.72	1.8 a	1.3		f
24	07°55′	89°20′	3581	0.62	1.8 a	1.1		f
25	06°59′	90°58′	3955	0.92	1.85n	1.70		f
26	08°42′	92°35′	3721	0.17	1.8 a	0.3		f
27	09°55′	91°47′	3791	0.12	1.8 a	0.2		f
28	10°35′	91°21′	3725	0.03	1.8 a	0.1		f
29	10°57′	91°07′	3763	0.55	1.8 a	1.0		f
30	11°32′	90°50′	3763	0.63	1.8 a	1.1		f
31	12°06′	90°42′	3673	0.46	1.8 a	0.8		f
32	12°17′	90°23′	4726	0.26	1.8 a	*0.5*		155
33	11°38′	89°58′	3632	0.80	1.8 a	1.4		f
34	11°02′	89°49′	3751	0.16	1.8 a	0.3		f
35	09°52′	89°23′	3556	0.03	1.8 a	0.1		f
36	10°23′	87°59′	3235	0.39	1.8 a	0.7		f
37	11°19′	87°37′	3744	0.50	1.8 a	*0.9*		90
38	10°41′	88°48′	3235	0.22	1.8 a	0.4		f
39	11°18′	89°11′	3577	0.42	1.8 a	*0.7*		125
40	10°41′	90°44′	3908	0.54	1.8 a	1.0		f
41	11°33′	92°28′	3864	0.15	1.8 a	0.3		f
42	12°08′	92°20′	3834	0.64	1.8 a	1.2		f
44	13°11′	92°05′	5311	0.57	1.8 a	*1.1*		117
45	13°40′	92°15′	2537	0.73	1.8 a	*1.3*		114
46	13°26′	93°06′	4510	0.79	1.8 a	*1.4*		120
47	13°05′	93°18′	3925	0.69	1.8 a	*1.3*		130
48	12°44′	93°27′	4001	1.37	1.8 a	2.5		f
49	12°19′	93°40′	4470	0.24	1.8 a	0.4		f
50	11°39′	94°00′	4126	0.15	1.8 a	0.3		f
51	10°34′	95°22′	4107	0.54	1.8 a	1.0		f
52	12°10′	95°29′	4211	0.41	1.8 a	0.7		f
53	13°06′	94°49′	4060	1.42	1.8 a	2.6		f
54	13°26′	94°32′	4063	1.10	1.86n	2.05		f
55	14°17′	94°30′	5115	1.82	1.9 a	3.5		f
56	14°04′	95°17′	4012	0.45	1.9 a	0.9		f
57	14°42′	95°33′	3444	1.90	1.9 a	3.6		f
58	15°28′	95°18′	2361	0.34	1.9 a	0.6		f
59	15°10′	96°18′	4707	0.72	1.9 a	1.4		f

(to be continued)

Table 1. (continued)

Station No.	Position		Water Depth, meters	Thermal Gradient	K	Q	Tilt	Penetration
	Latitude	Longitude		Average				
	N	W		$\times 10^3$ °C cm^{-1}	$\times 10^6$ cal °C^{-1} cm^{-1}sec^{-1}	$\times 10^6$ cal cm^{-2} sec^{-1}	Degrees	cm
60	13°52′	96°57′	3879	0.25	1.9 a	0.5		f
61	14°13′	97°30′	3634	0.26	1.9 a	0.5		f
62	13°45′	98°30′	3410	1.10	1.89n	2.07		f
63	14°29′	98°47′	3505	1.22	1.9 a	2.3		f
64	15°01′	98°54′	3522	0.53	1.9 a	1.0		f
65	15°41′	99°09′	4001	1.23	1.9 a	2.3		f
66	16°06′	99°35′	5363	0.72	1.9 a	1.4		f
67	16°01′	100°32′	4029	0.63	1.9 a	1.2		f
68	15°40′	101°03′	3627	2.98	1.9 a	5.7		f
69	14°51′	101°23′	3567	2.28	1.9 a	*4.3*		146
70	14°30′	102°03′	3535	0.75	1.80n	1.35		f
71	14°39′	103°22′	3228	1.40	1.8 a	2.5		f
72	17°27′	104°38′	3117	2.78	1.86n	5.08		f
73	18°13′	104°39′	4220	0.70	1.9 a	1.3		f
74	17°26′	107°24′	3625	2.37	1.9 a	4.5		f
75	16°21′	111°28′	3673	0.73	1.9 a	1.4		f
76	17°24′	112°42′	3382	2.52	1.9 a	4.7		f
77	16°30′	114°59′	4054	0.99	1.8 a	1.8		f
78	17°01′	116°22′	3936	1.68	1.8 a	3.0		f
79	18°24′	115°58′	3885	1.85	1.8 a	*3.3*		157
80	19°29′	115°02′	3663	0.37	1.8 a	0.7		f
81	18°58′	113°33′	3621	1.42	1.73n	2.45		f
82	20°56′	112°03′	3476	1.11	1.77n	1.94		f
83	21°10′	113°18′	3908	0.25	1.9 a	0.5		f
84	21°42′	114°24′	3448	3.06	1.9 a	5.8		f
85	22°20′	113°46′	4039	0.76	2.0 a	1.5		f
86	22°53′	113°20′	3711	1.56	2.0 a	3.1		f
87	23°22′	112°58′	3546	2.10	2.0 a	4.2		f
88	23°51′	112°49′	3213	2.20	2.0 a	4.4		f
89	24°31′	113°13′	3600	1.85	2.0 a	3.7		f
90	24°36′	113°44′	3592	1.88	2.0 a	3.8		f
91	24°25′	114°46′	3725	1.67	2.0 a	3.3		f
92	24°09′	116°02′	3810	0.86	2.0 a	1.7		f
93	25°04′	117°20′	3840	1.75	2.0 a	3.5		f
94	26°01′	118°30′	4272	0.36	2.0 a	0.7		f
95	26°46′	120°00′	4149	1.14	2.0 a	2.3		f
96	28°04′	120°30′	4111	1.68	2.0 a	3.4		f
Expedition T. Washington 65-1								
1	5°54′	79°53′	3075	2.08	1.8 a	3.7	15-30	f
1A	5°53′	79°53′	3214	1.96	1.8 a	3.5	0-15	f
5	12°18′	102°26′	3065	1.32	1.8 a	2.4		f
7	13°32′	105°43′	3445	1.17	1.8 a	2.1		f
Expedition Zetes								
110*	25°10′	149°21′	5405	0.52	2.07n	1.10	0-15	f
111*	26°42′	147°29′	5394	1.01	2.09n	2.10	0-15	f
112*	28°40′	144°55′	5031	0.70	2.11n	1.47	0-15	f

(to be continued)

Table 1. (continued)

Station No.	Position		Water Depth, meters	Thermal Gradient	K	Q	Tilt	Penetration
	Latitude	Longitude		Average				
	N	W		$\times 10^3$ °C cm^{-1}	$\times 10^3$ cal °C^{-1} cm^{-1}sec^{-1}	$\times 10^6$ cal cm^{-2} sec^{-1}	Degrees	cm
114*	30°12′	142°17′	5075	0.55	2.11n	1.13	0-15	f
115	31°01′	137°41′	4628	0.77	1.92n	1.48	0-15	f
116	31°00′	137°00′	4618	0.79	2.0 a	1.6	0-15	f
118	31°10′	135°57′	4584	0.75	1.89n	1.40	0-15	f
119	31°13′	134°01′	4689	0.87	1.9 a	1.7	0-15	f
120	31°18′	133°00′	4500	0.49	1.94n	0.95	0-15	f
121	31°24′	132°00′	4641	0.80	1.9 a	1.5	0-15	f
122	31°23′	131°03′	4541	0.44	1.91n	0.83	0-15	f
123	31°33′	129°58′	4714	0.89	1.9 a	1.7	0-15	f
124	31°40′	128°59′	4353	0.53	1.9 a	1.0	0-15	f
Expedition Tripod								
1	00°40′	84°36′	3003	1.75	2.0 a	3.5	0-15	f
2	01°38′ S	84°55′	2214	1.62	2.0 a	3.2	0-15	f
3	05°05′ S	86°01′	3768	0.74	2.0 a	1.5	0-15	f
4	02°00′ S	86°02′	2580	1.15	1.91n	2.20	0-15	f
5	01°53′	86°14′	2688	2.30	2.0 a	4.6	0-15	f
6	00°06′	87°00′	2664	0.66	2.0 a	1.3	0-15	f
7	01°53′ S	87°04′	2768	1.59	2.0 a	3.2	0-15	f
8	03°52′ S	87°01′	3535	1.47	2.0 a	2.9	0-15	f
10	00°54′	88°01′	2482	1.65	1.92n	3.2	0-15	f
11	01°51′	88°01′	2516	1.90	2.0 a	3.6	0-15	f
12	04°16′	88°51′	2328	0.23	2.0 a	0.7	0-15	f
13	05°02′	89°38′	2870	1.23	2.0 a	2.5	0-15	f
14	06°13′	90°50′	3626	0.58	2.0 a	1.2	0-15	f
15	07°45′	92°15′	3442	0.71	1.92n	1.36	0-15	f
16	08°53′	93°15′	3493	0.33	1.73n	0.59	0-15	f
17	09°22′	93°43′	3645	0.35	1.8 a	0.6	0-15	f
18	10°12′	94°26′	3848	0.37	1.75n	0.65	0-15	f
19	11°40′	95°23′	4141	0.37	1.77n	0.65	0-15	f
20	12°39′	96°22′	4035	0.32	1.81n	0.58	0-15	f
21	16°16′	101°17′	3465	1.57	1.8 a	2.8	0-15	f
22	15°34′	102°44′	3588	0.46	1.8 a	0.8	0-15	f
23	14°26′	108°24′	3782	1.40	1.74n	2.43	0-15	f
24	14°31′	109°04′	3520	1.96	1.8 a	3.5	0-15	f
25	14°30′	109°38′	3873	3.47	1.8 a	6.3	0-15	f
26	14°28′	111°50′	3607	1.93	1.73n	3.35	0-15	f
27	14°31′	112°46′	3822	1.11	1.8 a	2.0	0-15	f
28	15°38′	112°57′	3944	1.81	1.75n	3.18	0-15	f
29	16°47′	113°00′	3439	1.66	1.82n	3.03	0-15	f
30	17°30′	113°00′	3702	0.32	1.74n	0.55	0-15	f
31	18°08′	113°00′	3573	1.09	1.8 a	2.0	0-15	f
32	18°31′	113°00′	3523	1.78	1.8 a	3.2	0-15	f
33	19°06′	112°57′	3546	1.35	1.80n	2.43	0-15	f
34	20°15′	112°42′	3512	1.54	1.81n	2.79	0-15	f
35	20°35′	112°39′	3476	1.44	1.8 a	2.6	0-15	f
36	20°50′	112°31′	3596	0.24	1.85n	0.44	0-15	f
37	21°11′	113°00′	3623	0.75	1.9 a	1.4	0-15	f
38	20°45′	114°27′	3844	0.32	1.9 a	0.6	0-15	f

(to be continued)

Table 1. (continued)

Station No.	Position		Water Depth, meters	Thermal Gradient	K	Q	Tilt	Penetration
	Latitude	Longitude		Average				
	N	W		$\times 10^3$ °C cm^{-1}	$\times 10^3$ cal °C^{-1} cm^{-1}sec^{-1}	$\times 10^6$ cal cm^{-2} sec^{-1}	Degrees	cm
39	20°32′	114°58′	3703	1.10	1.9 a	2.1	0-15	f
40	20°21′	115°59′	4098	0.44	1.9 a	0.8	0-15	f
41	20°38′	116°53′	3911	1.06	1.9 a	2.0	0-15	f
42	20°48′	118°01′	4026	0.57	1.94n	1.11	0-15	f
43	20°54′	119°00′	4084	1.28	2.0 a	2.6	0-15	f
44	21°20′	119°20′	4186	0.40	2.0 a	0.8	0-15	f
45	22°27′	119°10′	4122	0.99	2.01n	1.99	0-15	f
46	23°19′	119°00′	4022	0.56	2.00n	1.12	0-15	f
47	24°25′	118°46′	4193	0.70	2.0 a	1.4	0-15	f
48	25°58′	118°26′	4204	0.27	2.05n	0.55	0-15	f
49	26°47′	118°17′	4079	0.72	2.1 a	1.5	0-15	f
50	27°48′	118°08′	3692	0.67	2.19n	1.47	0-15	f
51	28°15′	118°04′	4116	0.37	1.98n	0.73	0-15	f

* Stations listed but not appearing on chart.

Note: Stations with thermal conductivity measured on core are indicated by two figures after the decimal point, and stations with estimated conductivity by one figure after the decimal point. Stations with partial penetrations are underlined.

a indicates an estimated conductivity value.

n indicates a conductivity value determined from a gravity core.

f indicates full penetration.

S indicates southern latitude.

liability, the magnitude of the measurement errors caused by instrumental and environmental effects must be known. The magnitude of such errors can be estimated only if repeated determinations of the heat-flow have been made under the same conditions in the same area. Unfortunately, repeated observations have very seldom been made at the same position at sea. However, Lee and Uyeda (1965) have obtained a general estimate of the magnitude of the measurement errors by analyzing repeated and closely spaced stations. Fig. 1 presents Fig. 2 of their paper, the histogram of $(x_i - y_i)$ for pairs of heat-flow stations less than 10 km apart with heat-flow values x_i and y_i; (a) represents land data, and (b) oceanic data. Lee and Uyeda (1965) find a standard deviation of 0.47 for the 49 pairs of oceanic heat-flow stations considered in the analysis. On land if the heat-flow variations within 10 kms were due to some geological effects (e.g. volcanism), these were excluded from the analysis. This has not been done at sea. Consequently the histogram for oceanic values represents the scatter due to measurement error superposed upon

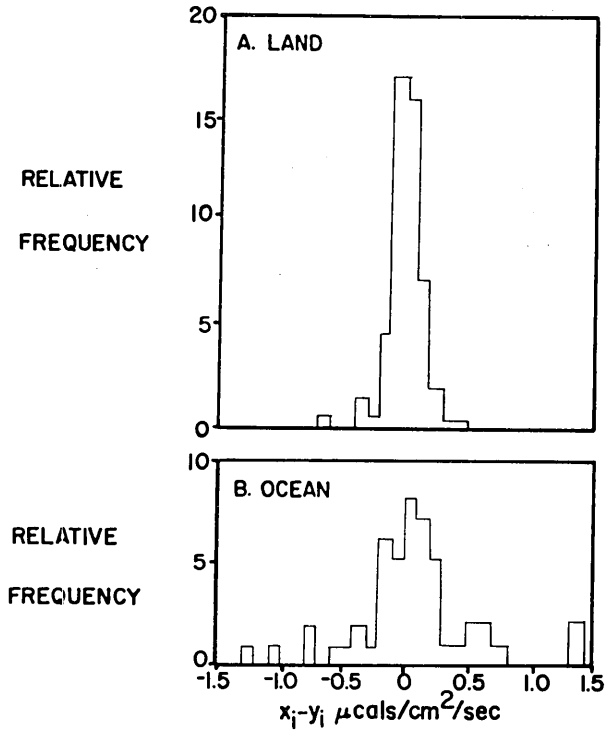

Fig. 1. Histogram of $(x_i - y_i)$ for pairs of heat-flow stations less than 10 km apart with heat-flow values x_i and y_i, (a) for land data, and (b) for oceanic data (Lee and Uyeda, 1965).

a random scatter due to real geological effects. Ignoring the random scatter, Fig. 1 suggests that the scatter due to experimental error alone is more likely to be 0.35 μcal/cm^2/sec than 0.47 μcal/cm^2/sec. Hence for Fig. 2 a contour interval of approximately three times this standard deviation; i.e., 1 μcal/cm^2/sec was chosen.

The contouring was done by hand and due consideration was paid to the bathymetry and magnetics of the whole region. Where the heat-flow data are relatively sparse, the contour lines have been drawn parallel to the bathymetry. For example around the East Pacific Rise between 10° and 20°N the contours have been drawn north-south. They could equally well have been drawn east-west.

4. Discussion of the Results

Fig. 3 presents an outline of the East Pacific Rise and the con-

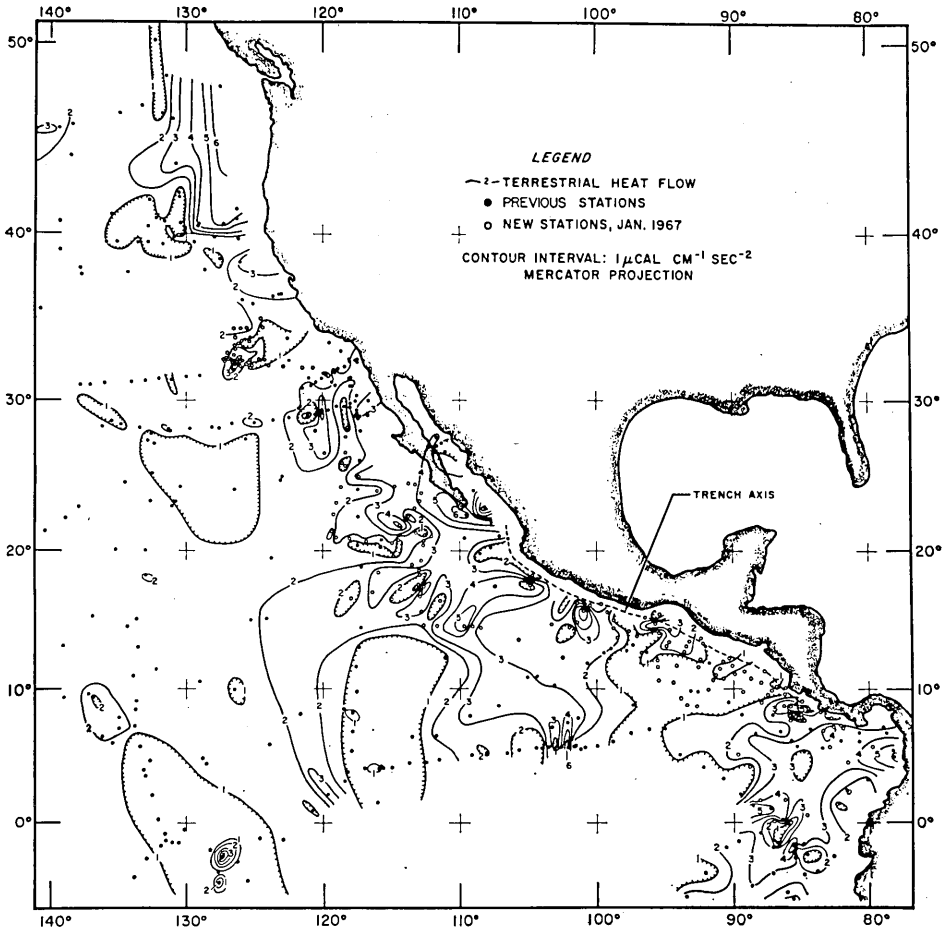

Fig. 2. Contour chart of heat-flow in the eastern Pacific. Contour interval 1 μcal/cm^2/sec.

spicuous areas of faulted topography associated with it. A comparison of this figure and Fig. 2 indicates one striking feature: while most of the heat-flow values to the west of the Rise are around normal, across the Rise and to the east of it the values vary widely. The variations are both large and consistent. Wide-spread areas of high and low heat-flow are intermixed. As the area covered by the contour chart is so extensive and the heat-flow values so varied, the area has been divided into three main regions for more detailed discussion. The boundaries of the regions roughly correspond to the three main bathymetric provinces covered by the chart. The nomenclature of the bathymetric provinces

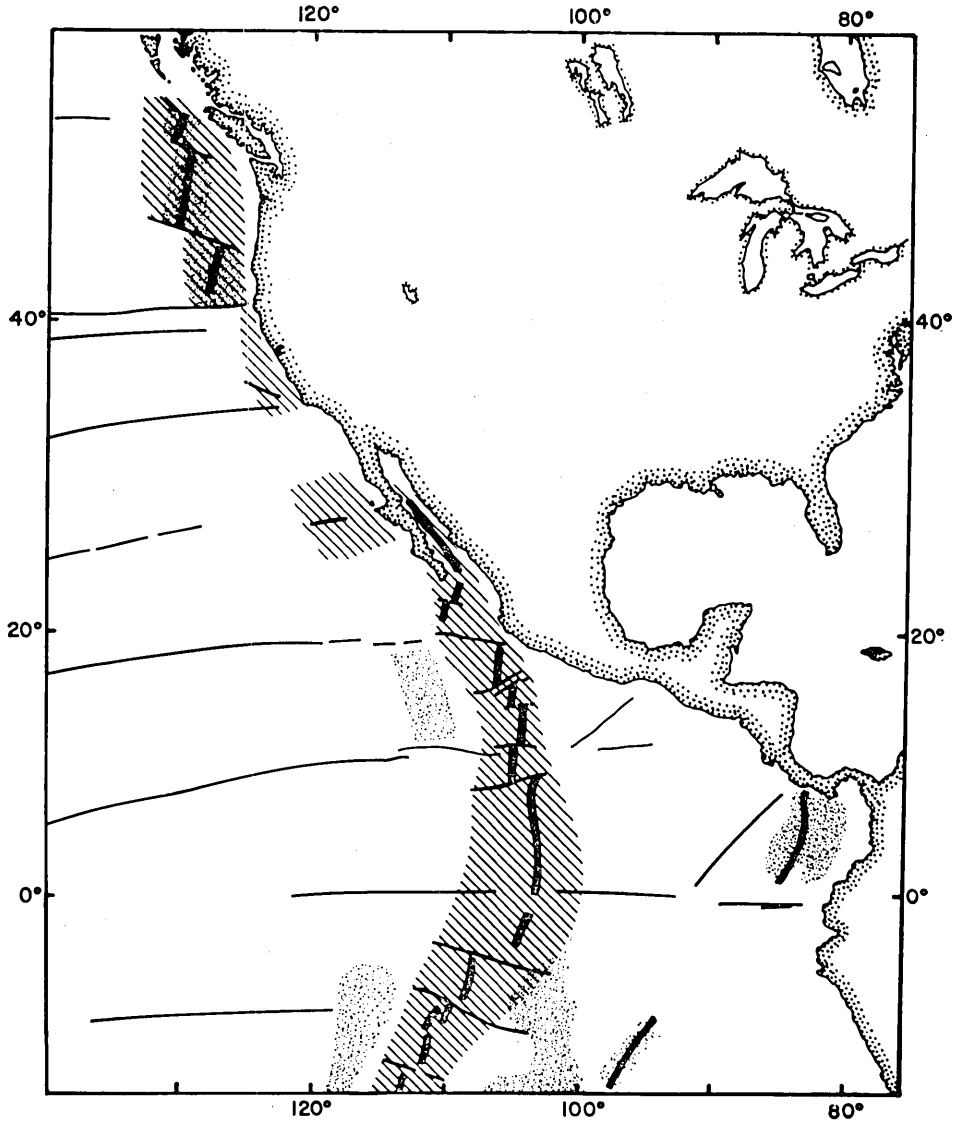

Fig. 3. An outline of the conspicuous areas of faulted topography associated with the East Pacific Rise (Menard, in press).

NOTE: The thick black lines represent the crest and the shaded area the flanks of the Rise. The thin black lines trace the other fracture zones. The dotted regions outline other areas of rough topography.

described in this paper is that of Chase and Menard (1965) and Vine (1966).

(a) The region north of 25°N. This region which encompasses the Mendocino and Murray Fracture Zones and the Mason-Raff (1961) magnetic lineations has two small areas showing a high density of heat-flow stations. In March 1965, during the first deep-sea testing of the Scripps deep-sea ocean-bottom magnetometers, 35 measurements were taken between 125°W and 127°W and 32°N and 34°N. This region encloses a large negative and a large positive north-south trending Mason-Raff (1961) magnetic lineation. The heat-flow measurements were located so as to test whether the magnetic signature could be correlated with differences in the surface heat-flow. It could not. Apart from two low values, the heat-flow measurements were all around 2.0 μcal/cm^2/sec and they showed no systematic variation. This is not surprising if the age of the anomalies is pre-Jurassic as suggested by Vacquier *et al.* (1961).

Further north, the contour chart emphasizes quite strikingly the sharp change in heat-flow seen where the Gorda Ridge intersects the Mendocino Fracture Zone. Menard (1965) has suggested that this ridge may be a north-south extension of the East Pacific Rise. The high heat-flow values on its crest and the rapid drop in value to both the south and west add weight to his suggestion.

(b) The area west of 100°W and south of 25°N. This region encompasses the East Pacific Rise, the Gulf of California, the Mathematician Seamounts, the Clarion and Clipperton Fracture Zones, the California Seamount Province, as well as a large section of the Pacific Basin. Apart from two areas of low heat-flow, the values to the west of the East Pacific Rise, are all about or just below the oceanic average. This is similar to the greater part of the Pacific Ocean and to other oceanic basin areas which have uniformly normal heat-flow. To the north, in the Baja California Seamount Province, where there is no Rise between the deep ocean and the continent, there is a definite increase in the outward flow of heat as one approaches the Californian coast. This suggests that not only Guadalupe Island but many of the seamounts in this area may be relatively recent in origin. To the south of the Seamount Province lie the Molokai, the Clarion, and Clipperton Fracture Zones. A comparison of Figs. 2 and 3 indicate that none of these fracture zones to the west of the East Pacific Rise has any obvious relation to the distribution of heat-flow values. Where these zones intersect the Rise, there are too few values to determine whether or not the

fracture zones have any observable effect. The very high heat-flow and the low magnetic relief across the Mathematician Seamounts suggest that they are formed over a 200—300 km-wide, north-south running region of anomalously high temperature at very shallow depths. The shallowness of the 500°C isotherm may account for the lack of magnetic relief though, on the other hand, the low relief could be caused by the remanent magnetism of the intrusive magma being no different from the surrounding rock. To the east of these seamounts lies the East Pacific Rise. The scarcity of data across the Rise is caused by the extreme small-scale roughness of the topography; one heat-flow instrument was lost during expedition Papagayo in an unsuccessful attempt to obtain an east-west profile across it. Where heat-flow values do exist, they are generally high, though on the profile across the Rise completed on expedition Risepac by Von Herzen and Uyeda (1963) large-scale, very localized, variations of heat-flow were found. Our new values in this area confirm the conclusion of these authors that the East Pacific Rise has a broad heat-flow maximum two to three times the oceanic average. Superposed upon this are large local variations probably atributable to localized magmatic intrusions to shallow depths.

(c) The area east of 100°W. This area comprises the Middle America Trench, the Guatemala Basin, the Cocos and Carnegie Ridges and the Galapagos Rise. It is bounded to the west by the East Pacific Rise and to the east by the continent of South America. During expeditions Tripod and Papagayo many heat-flow stations were taken in this area. Fig. 4, a plot of heat-flow values against distance from the Middle America Trench axis, as defined by Fisher (1961), indicates no significant decrease in the outward flow of heat in the trench.

Most heat-flow values in the Guatemala Basin are below normal. The mean heat-flow for the 32 values in the area bounded by the 12° and 2° lines of latitude and the 100° and 90° lines of longitude is 0.79 μcal/cm^2/sec. The mean has a standard deviation of 0.45 and a standard error of 0.08 μcal/cm^2/sec. To test whether this small mean value could have arisen through oversampling of a small region of very low flow, the 10° square was divided into twenty-five 2° squares. The mean heat-flow in the 14 of these squares which had values being within their boundaries was evaluated. They have a mean of 0.84 μcal/cm^2/sec with a standard deviation of 0.38 and a standard error of 0.11. These figures are in good agreement with those determined from the raw data. The Guatemala Basin is an area of low heat flow. The flow is significantly

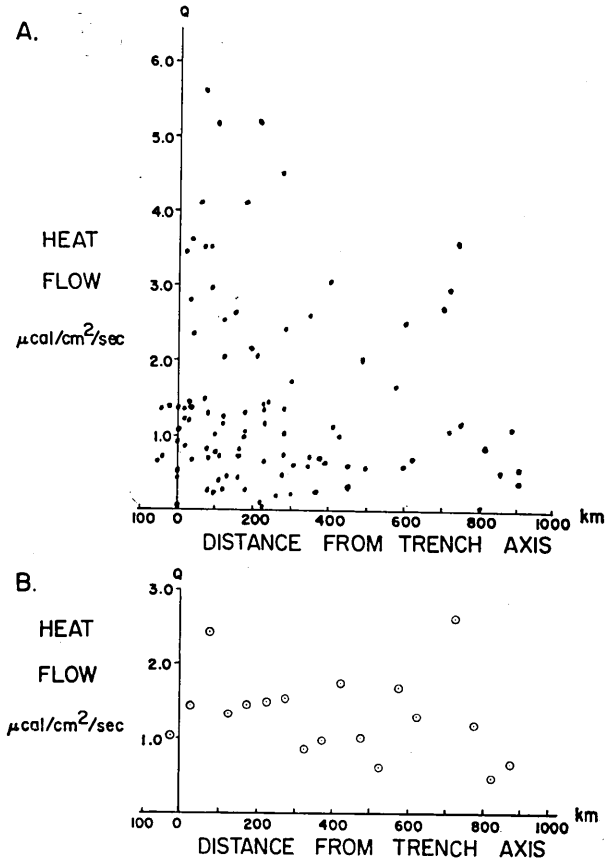

Fig. 4. Plot of heat-flow values versus distance from the axis of the Middle America Trench, (a) raw values, and (b) values averaged in 50 km intervals.

less than (a) the oceanic average of 1.58 μcal/cm^2/sec (Lee and Uyeda, 1965) and (b) the mean flow through ocean basins of 1.28 μcal/cm^2/sec (Lee and Uyeda, 1965). The area of low heat-flow is 1,000 kms wide and at least 1,000 kms long. The exact length is not known as there are no values between 2°N and 10°S. This large area of low flow bounded on two sides by regions of two or three times normal flow is one of the most striking features of the whole area. It is difficult to explain such a wide-spread area of subnormal heat-flow by any of the present hypotheses concerning ocean heat-flow. Perhaps the mantle beneath the region is deficient in heat sources.

Southeast of this region of low heat-flow lie the Cocos Ridge, the

Galapagos Platform, the Carnegie Ridge and the area between these ridges and the coast of Central and South America. These ridges, according to Menard (1965), are branches of the East Pacific Rise. The whole region except for the Galapagos Platform and the Carnegie Ridge is one of high heat-flow, with an average value greater than 3 μcal/cm^2/sec near the Isthmus of Panama. The region between the Galapagos Platform and the Carnegie Ridge and the Cocos Ridge is one of uniformly high heat-flow. Values of more than 4 μcal/cm^2/sec have been reported in this small area by Von Herzen and Uyeda (1963), Lamont (unpublished) and in this paper. These very high values appear directly related to a large 1500 gamma negative magnetic anomaly running east-west between the two ridges. This large negative anomaly (Raff personal communication) can be explained by an east-west normally magnetized intrusion. The high heat-flow values suggest recent intrusion.

To the west of the East Pacific Rise, the heat-flow measurements take on the characteristic values of a normal deep ocean basin, while those over and to the east of the Rise show considerable variation. This variation indicates that the whole region off the coast of North and Central America is geothermally anomalous.

Thermal convection in the mantle offers a simple explanation of the heat-flow structure across the East Pacific Rise. Hot material ascending under the crest and moving horizontally away from it can account for the broad band of high heat-flow found across the Rise. The isolated regions of very high flow near the crest can be attributed to recent local intrusions formed by the upward movement of magma. While this hypothesis adequately explains the observed variation of heat-flow across the Rise, it runs into difficulty in accounting for the distribution of heat-flow in the Guatemala Basin, the Middle America Trench and on the Cocos Ridge. Menard (1965) has suggested that crustal blocks moving east from the crest of the Rise and being pushed against Central America could form the Tehuantepec Ridge, the Guatemala Basin and the Middle America Trench. He proposes a thermal convection cell arising under the East Pacific Rise to explain the lateral movements of these blocks. However, if thermal convection is the driving mechanism, one would expect to find lower than average heat-flow where these blocks descend beneath the continents. East of the Rise where the blocks descend under the Middle America Trench, the heat-flow should be subnormal. This is not the case. Fig. 4 shows that there is no appreciable decrease in the outward flow of heat across the Trench.

The wide-spread area of low flow through the Guatemala Basin presents another difficulty to Menard's hypothesis. To explain the low heat-flow in this basin and the adjacent high values it is necessary to postulate another convection cell centered on the Cocos Ridge. However, (a) the position of the Middle America Trench relative to the East Pacific Rise and the Cocos Ridge and (b) the lack of any evidence of crustal downwarping in the Guatemala Basin makes this explanation of the large area of low heat-flow unlikely. Though the depth to the Mohorovičic discontinuity in the Guatemala Basin is anomalously shallow for the oceans (Shor and Fisher, 1961; Raitt personal communication), the relatively small radiogenic heat content of the oceanic crust makes it equally improbable that this area of low flow can be accounted for by crustal thinning. One is thus forced to conclude that only a mantle deficient in radioactive heat sources can explain the wide-spread area of low heat-flow. It is difficult to suggest a mechanism that might account for this deficiency.

Bullard (1964) has suggested that the differentiation of the rocks within the mantle might explain the similarity of the mean heat-flow on land with the oceanic mean. In the course of this differentiation, the uranium, thorium and potassium have been concentrated in the continental crust, while under the oceans the same amounts have remained spread through a greater range of depth. This hypothesis proposes that the mantle immediately beneath the continents has a lower concentration of radioactive minerals than that beneath the oceans. If, at some time in the past, the continental crust alone were to move, a mantle deficient in radioactive minerals would be left behind. Such a mechanism is a possible explanation of the low heat-flow in the Guatemala Basin. If the continent of Central America had originally been situated above the Basin and had then moved northward, it might have left behind a continental-type mantle. This being deficient in radioactive minerals would have a radiogenic heat output lower than that of the normal oceanic mantle. Another possible explanation of the deficiency of radioactive minerals is that instead of differentiating vertically they may have separated laterally. If these minerals had accumulated in the mantle beneath the Cocos Ridge at the expense of the mantle beneath the Guatemala Basin, this might account for the deficiency of heat sources beneath the Basin. It must be pointed out, though, that the last two hypotheses are both highly speculative and suffer the disadvantage that there is no adequate mechanism explaining horizontal

differentiation of the mantle.

5. Instrumental Details

(a) Temperature gradient measurements. The temperature gradients through the ocean floor on Argo 3-65 were all measured with a probe 2 m long and 2.0 cm in diameter. This probe, the recorder and pressure case were essentially the same as those described by Von Herzen, *et al.* (1962). Towards the end of this cruise both instruments of this type were lost and for the following expedition, Papagayo, a new instrument was designed (Corry, *et al.*, in preparation). Basically, the instrument consists of three temperature-sensitive elements located one meter apart inside a probe, 2.3 m long and 2.0 cm in diameter. The record of temperature versus time of these elements is made by a recorder carried above the probe. A fourth temperature-sensitive element, located at the top of the recording case, measures the absolute water temperature. The thermal conductivity of the surrounding sediment is measured at the same time as the temperature gradient by heating a thin probe attached by a slider to the main probe. This probe, which is mounted externally to the main probe, also measures the depth of penetration and takes a small core of the sediment. The conductivity needle is electrically connected to the recorder by a retracting cable. This new instrument was used during the Papagayo, T. Washington 1, Zetes and Tripod expeditions. More than 250 successful heat-flow stations have been made with it.

It has been suggested that some of the variation of heat-flow values might be caused by fluctuations in the bottom-water temperature, recent slumps and recent sharp changes in sedimentation rates. Such changes should show up as changes of temperature gradient in the vertical direction. The third thermistor was added to the probe to test whether such changes of gradient did exist and how wide-spread they were. On only three of the stations reported in this paper, Papagayo—3, Zetes—115 and Tripod—3, did the temperature difference between the middle and upper thermistors in the probe disagree by more than 0.2×10^{-3}°C with that between the middle and lower. Of these stations only Zetes—115 has a difference of greater than 0.3×10^{-3}°C. A difference of less than 0.2×10^{-3}°C in a normal gradient of 0.7×10^{-3}°C is not considered significant as such a difference could arise through a summation of reading errors and a real vertical change of thermal conductivity in the sediment. Thus our present stations indicate that, in the Pacific, large

changes in temperature gradient in the near-surface layers of the ocean sediment are not wide-spread. This confirms the conclusion that Langseth, *et al.* (1967) reached for the near-surface sediment layers in the Atlantic.

The new instrument has a tiltmeter which enables one to determine approximately the angle of penetration, the calibration scales being offset by different amounts should the tilt be between 15° and 30° or >30°. The slider on the side of the probe enables the depth of penetration to be determined on partial penetrations. The distance of the one-way slider from the bottom of the probe gives the distance penetrated. Stations showing a partial penetration, where the probe did not penetrate far enough to cover the uppermost thermistor, are underlined in Table 1.

(b) Thermal conductivity measurements. The thermal conductivities presented in Table 1 were determined using a value measured from sediments in a core taken either at or very near the temperature gradient measurement. The measurements on the cores were carried out by the needle probe technique (Von Herzen and Maxwell, 1959). When no core was taken at a station, the conductivity was assumed as being the weighted average of those from nearby stations. During expeditions Zetes and Tripod it was hoped to make many *in situ* measurements but, unfortunately, owing to difficulties with underwater connectors, only two successful *in situ* measurements were made in this area, both on the last leg of expedition Zetes. The mean of these measurements proved more than 10% greater than the mean of 1.95 cal/cm/sec/°C determined by the transient needle probe method on cores taken at the same stations. These *in situ* measurements were disregarded in the present paper as more experiments are needed to test the validity of the method. Tests at present being carried out at Scripps Institution of Oceanography tend to confirm the *in situ* measurements.

6. Acknowledgements

This research was supported by the National Science Foundation under grants NSF GM 7 and NSF GP 3791 and also by the Office of Naval Research. We would like to thank Captain Phinney and the crew of the R/V ARGO, and Captain Hansen and the crew of the R/V THOMAS WASHINGTON for their splendid cooperation at sea. Also we would like to thank the members of the scientific parties on board these ships during the various expeditions, especially Mr. F. S. Dixon who took many of the measurements and whose many comments were often in-

valuable in the design and safety of the apparatus. We are further indebted to Dr. H. W. Menard and Dr. P. Rudnick who critically reviewed this manuscript. Some unpublished Lamont values were taken into consideration in the construction of the contour chart. We are grateful to Dr. M. G. Langseth for letting us see his results prior to publication.

References

BULLARD, E. C., "The flow of heat through the floor of the Atlantic Ocean", *Proc. Roy. Soc. London*, [A], **222**, 408-429, 1954.

BULLARD, E. C., A. E. MAXWELL, and R. REVELLE, "Heat flow through the deep sea floor", *Advan. Geophys.*, **3**, 153-181, 1956.

BULLARD, E. C., "The flow of heat through the Earth", *I. C. S. U. Rev. World Sci.*, **6**, 78-83, 1964.

CHASE, T. C. and H. W. MENARD, *Bureau of Commercial Fisheries, topographic charts no. 1-23*, (Bureau of Commercial Fisheries, Dept. of Interior, Washington, D. C., 1965).

CORRY, C. E., C. DUBOIS, and V. VACQUIER, "Instrument for measuring terrestrial heat flow through the ocean floor", paper submitted to *J. Mar. Res.*, March 1967.

FISHER, R. L., "Middle America Trench: Topography and structure", *Bull. of the Geol. Soc. Amer.*, **72**, 703-720, 1961.

FOSTER, T., "Heat-flow measurements in the north-east Pacific and in the Bering Sea", *J. Geophys. Res.*, **67**, 2991-2993, 1962.

LANGSETH, M. G., P. J. GRIM, and M. EWING, "Heat-flow measurements in the east Pacific Ocean", *J. Geophys. Res.*, **70**, 367-380, 1965.

LANGSETH, M. G., L. Le PICHON, and M. EWING, "Crustal Structure of the mid-ocean ridges 5. Heat flow through the Atlantic Ocean floor and convection currents", *J. Geophys. Res.*, **71**, 5321-5355, 1966.

LEE, W. H. K., and S. UYEDA, "Review of heat flow data", in *Terrestrial Heat Flow*, edited by W. H. K. Lee, Geophysical Monograph No. 8, (Amer. Geophys. Union, 1965), 87-190.

MASON, R. G., and A. D. RAFF, "Magnetic survey off the west coast of north America, 32°N latitude to 42°N latitude", *Bull. Geol. Soc. Am.*, **72**, 1259-1266, 1961.

MAXWELL, A. E., "The outflow of heat under the Pacific Ocean", Umpublished Ph. D. dissertation, University of California, Los Angeles, Calif., 1958.

MENARD, H. W., "Marine geology of the Pacific", (McGraw-Hill Book Co., New York, 1965).

MENARD, H. W., "Some remaining problems in sea floor spreading", in press.

SHOR, G. G., Jr. and R. L. FISHER, "Middle America Trench: Seismic refraction measurements", *Bull. Geol. Soc. Am.*, **72**, 721-730, 1961.

VACQUIER, V., S. UYEDA, M. YASUI, J. SCLATER, C. CORRY, and T. WATANABE, "Studies of the thermal state of the Earth 19th paper, Heat-flow measurements in the northwestern Pacific", *Bull. Earthq. Res. Inst.*, **44**, 1519-1535, 1967.

VINE, F. J., "Spreading of the ocean floor: New evidence," *Science*, **154**, 1405-1415, 1966.

VON HERZEN, R. P., "Heat-flow values from the southeastern Pacific", *Nature*, **183**, 882-883, 1959.

VON HERZEN, R. P., "Pacific Ocean floor heat-flow measurements, their interpretation and geophysical implications", Ph. D. dissertation, University of California, Los

Angeles, Calif., 1960.
VON HERZEN, R. P., "Geothermal heat flow in the Gulfs of California and Aden", *Science*, **140**, 1207-1208, 1963.
VON HERZEN, R. P. and A. E. MAXWELL, "The measurement of thermal conductivity of deep sediments by a needle probe technique", *J. Geophys. Res.*, **64**, 1557-1563, 1959.
VON HERZEN, R. P. and S. UYEDA, "Heat flow through the eastern Pacific Ocean floor", *J. Geophys. Res.*, **68**, 4219-4250, 1963.

---

22. 地球熱学 第21報 東太平洋海域の地殻熱流量

スクリプス海洋研究所 Victor VACQUIER, John SCLATER, Charles CORRY

スクリプス海洋研究所では，北米，中米沖に新たに197点の海洋底地殻熱流量の測定を行ない，従来の367点を加えて，西経140° 以東の南緯10° より北緯60° におよぶ海域において地殻熱流量の地域的分布を吟味した．この結果，東太平洋は，1) 北緯25° 以北のMason—Raffの地磁気縞状帯を含む海域，2) カルフォルニア海山地帯，東太平洋海嶺，カルフォルニア湾，東太平洋海盆等を含む海域，3) 中央アメリカ海溝，ココ，ガラパゴス，カーネギーの海嶺，ガテマラ海盆などの西経100° 以東の海域の3海域に大別される．2)，3) の海域においては，いくつもの大きな面積を占る平均3.0 μcal/cm^{2}sec 以上の高熱流量帯が，同規模の世界平均(1.58 μcal/cm^{2}sec) 以下の低流量帯と隣接して存在しており，北西太平洋海盆等の他の深海盆における一様な地殻熱流量の分布と著しい対照をなしている．東太平洋海嶺以東のこの高低熱流量の分布を大規模なマントル熱対流核で説明することは困難であるように思われる．
